Subdwarfs and white dwarfs from the *2MASS*, *Tycho-2*, *XPM* and *UCAC3* catalogues

George A. Gontcharov,[1] Anisa T. Bajkova,[1]
Peter N. Fedorov,[2] and Vladimir S. Akhmetov[2]

[1]Central astronomical observatory at Pulkovo of RAS,
Pulkovskoye chaussee 65/1, 196140, Saint-Petersburg, Russia.
[2]Institute of Astronomy of Kharkiv National University,
Sums'ka 35, 61022 Kharkiv, Ukraine

Abstract

The photometry from 2MASS, UCAC3 and SuperCosmos catalogues together with the proper motions from the Tycho-2, XPM and UCAC3 catalogues are used to select the all-sky samples of 34 white dwarfs, 1996 evolved and 7769 unevolved subdwarfs candidates for R from 9 to 17 magnitude. The samples are separated from the main sequence with admixture less than 10% owing to the detailed analysis of the distribution of the stars in the different color index (CI) vs. reduced proper motion (RPM) diagrams for various latitudes with special attention to the estimation of admixtures in the samples and with Monte-Carlo simulation. It is shown that the XPM and UCAC3 have the same level of proper motion accuracy. Most of the selected stars has at least 6-band photometry with accuracy is proved to be better than 0.2. The multi-color photometry allows us to eliminate some admixtures and reveal some binaries. The empirical calibrations of absolute magnitude versus CI and RPM for Hipparcos stars give us photometric distances and 3D distribution for all the stars. Although the selection method and uneven distribution of the XPM and UCAC3 data provide noticeable biases the preliminary conclusions are made. The subdwarfs show some concentration to the galactic centre hemisphere with voids because of extinction in the Gould belt and galactic plane. Some yet unexplained overdensities of the evolved subdwarfs are seen in several parts of the sky. For 183 stars with radial velocities 3D motion and galactic orbits are calculated. For 56 stars with Fe/H collected from various sources we find the relations of the metallicity with CI, asymmetric drift velocity and orbital eccentricity. It is shown that most unevolved subdwarfs belong to the halo with the scale height of 8 ± 1 kpc and local mass density of halo subdwarfs of $2\cdot10^{-5} M_{\odot}\ pc^{-3}$. Most evolved subdwarfs belong to the thick disk with the scale height of 1.25 ± 0.1 kpc. Main parameters of the selected stars are compiled into new SDWD catalogue for future investigations. Special attention should be paid to spectroscopic observations of these stars because 53% of the selected white dwarfs, 94% of evolved and 98% of unevolved subdwarfs are now classified for the first time whereas the existed spectral classification is wrong in many cases.

1 Introduction

Distribution, kinematics, age-velocity (AVR) and age-metallicity (AMR) relations of the subluminous stars, such as subdwarfs (SD) and white dwarfs (WD), are important yet poorly known data to study the structure, formation and history of the Galaxy. Unfortunately, a hard work of spectroscopic detections, classifications and measurements of the stars have been made for only hundreds of them at best and naturally sometimes are erroneous.

New all-sky astrometric and photometric surveys of millions stars, such as Tycho-2 [Høg et al., 2000], UCAC3 [Zacharias et al., 2009], 2MASS [Skrutskie et al., 2006], XPM [Fedorov, Myznikov & Akhmetov, 2009], become a good source to select large samples of the subluminous stars. This new spectroscopy-independent look on the stars is possible by use of multi-color photometry and its combination with proper motions known as *the reduced proper motions* (RPM). It is determined for the 2MASS Ks photometric band (and similar to others) as

$$M'_{Ks} = Ks + 5 + 5\lg(\mu) \tag{1}$$

where μ is a total proper motion in arcsec yr^{-1}. The interstellar extinction A_{Ks} should be added to the right part of this equation to make M'_{Ks} being an analog of the absolute magnitude M_{Ks}. But an advantage of the use of the 2MASS infra-red (IR) photometry is negligible value of A_{Ks} for the nearest part of the Galaxy: $A_{Ks} \approx 0.1A_V$. Consequently, 2MASS been the only current all-sky source of the precise IR photometry is ultimate for such investigations.

As shown by an intensive Monte-Carlo simulation [Gontcharov, 2009a] (hereafter GG2009), M'_{Ks} can be used instead of absolute magnitude M_{Ks} to select some classes of stars and calculate their *photoastrometric* distances via empirical calibration

$$M'_{Ks}\ vs.\ M_{Ks} \tag{2}$$

which is comparable to their *photometric* distances via calibration

$$(J - Ks)\ vs.\ M_{Ks} \tag{3}$$

Then one can consider stellar 3D distribution and kinematics. GG2009 proves that the introduced biases can be taken into the account by Monte-Carlo simulation.

The first investigation of SDs by use of the RPM was made by [Jones, 1972]. Some approaches in the current paper are similar to the ones in [Gontcharov, 2008b] where the RPM were used for the selection and study of clump red giants. The selection of a admixture-free sample of SDs from the Tycho-2 by RPM and a color index was proposed by GG2009. A noticeable investigation of the SDs from the SDSS survey [Finlator et al., 2000] in *a part of the sky* is made by [Smith et al., 2009].

As discussed later, the white dwarfs are a by-product of this selection of the SDs because sometimes these two classes could not be easy separated. Thus, we put more attention to the SDs.

2 Subdwarfs

There are several definitions of SD depending mainly on the research method. From the stellar evolution point of view they are the stars slightly hotter (bluer) than solar metallicity zero-age main sequence (ZAMS) or solar metallicity zero-age horizontal branch (ZAHB) stars of the same mass because of their lower-than-solar metallicity. From the spectroscopic point of view they are the stars slightly fainter than ZAMS and ZAHB of the same spectral class. From the photometric point of view they are the stars in the well-defined respectively unpopulated domain in a color-magnitude diagram. From the kinematic point of view they are the stars with large motion with respect to the Sun because all or majority of them are believed to belong to the galactic population II. One could show that no way to unite all

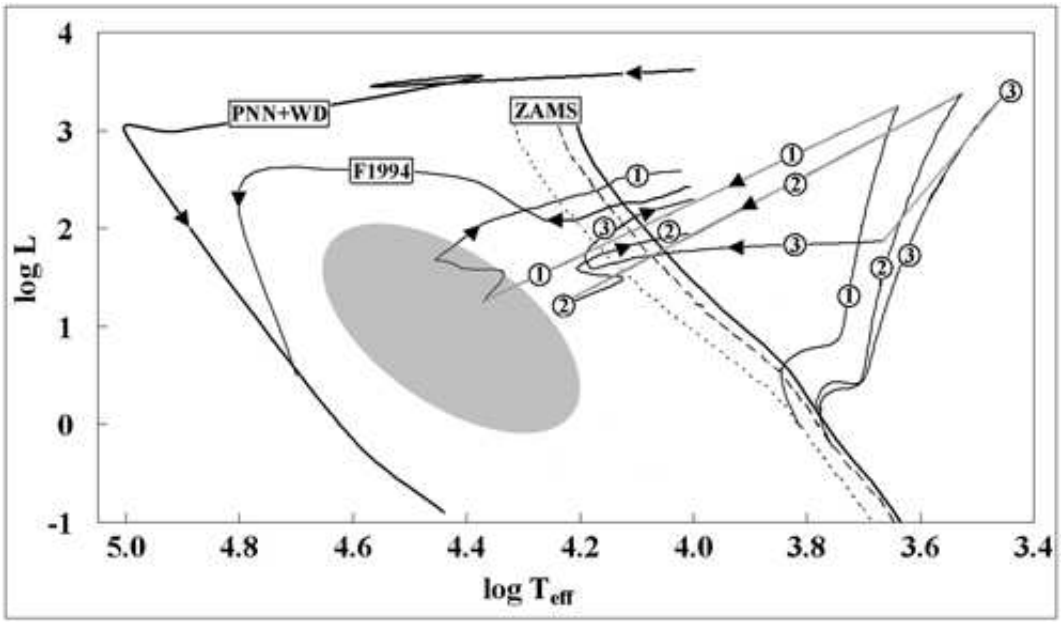

Figure 1: lg T_{eff} vs. lg L for ZAMS with $Z = 0.019$, 0.008 and 0.0004 — thick, dashed and dotted lines marked as ZAMS; PNN+WD track for $0.9M_{\odot}$, $Z = 0.004$ — thick line at left marked as PNN+WD; PNN+WD track from [Fagotto et al., 1994] for $0.5M_{\odot}$, $Z = 0.05$, $Y = 0.35$ marked as F1994; and 3 evolutionary tracks for stars of $0.9M_{\odot}$ before and $0.5M_{\odot}$ after helium flash, marked as 1, 2, 3 for $Z = 0.0004$ with $Y = 0.23$, $Z = 0.008$ with $Y = 0.25$ and $Z = 0.04$ with $Y = 0.46$ respectively. The grey ellipse shows the domain of subdwarfs generated after evolution in close binaries.

these definitions, first of all, because new investigations reveal some stars that fit only part of these criteria. Particularly, as shown later, not all SDs have low metallicity and population II kinematics.

We look at the SDs from the photometric-kinematic point of view selecting them as all the stars in a domain on color-RPM "$(J-Ks)$ – M'_{Ks}" diagram (in addition to the color-absolute magnitude "$(J - Ks)$ – M_{Ks}" diagram for some of the SDs). Therefore, we do not pay attention to the classic spectroscopic classification of SDs into sdO, sdB, etc.. Consequently, the selected samples can be considered as SD and WD *candidates* for spectroscopy. But even without spectroscopy this method allows us to consider the distribution of the samples on colors, spectral classes, velocities, metallicities, ages, galactic populations, and so on.

The position of some SDs in the effective temperature - luminosity ("lg T_{eff} – lg L") diagram is shown in Fig. 1. The solar metallicity ZAMS is shown as a thick line as well as the ones for $Z = 0.008$ and $Z = 0.0004$ are shown as dashed and dotted lines respectively and marked as "ZAMS" [Girardi et al., 2000]. As an example, three evolutionary tracks are shown by numbered thin lines (with jumps from the helium flash to ZAHB shown by grey):

1. $Z = 0.0004$, $Y = 0.23$, $M = 0.9M_{\odot}$ before and $M = 0.5M_{\odot}$ after helium flash [Girardi et al., 2000],
2. $Z = 0.008$, $Y = 0.25$ and the same masses [Girardi et al., 2000],
3. $Z = 0.04$, $Y = 0.46$ and the same masses [Bertelli et al., 2008].

Such tracks crossing solar ZAMS twice (deviating from ZAMS and ZAHB) are possible only in models with convective overshooting and never exist in the classical ones. Some models allow such considerable mass loss from $0.9M_\odot$ to $0.5M_\odot$ at the red giant branch (RGB) and its tip with helium flash [Cassisi et al., 2003]. But even a star with less mass loss, from $0.7M_\odot$ to $0.5M_\odot$ can be a SD [Girardi et al., 2000]. A classic stellar evolutionary track for planetary nebula nucleus (PNN) stage and white dwarf (WD) sequence with helium burning, $M = 0.9M_\odot$, $Z = 0.004$ is also shown as a thick line at high T_{eff} marked as "PNN+WD" [Vassiliadis & Wood, 1994]. Another PNN-WD track from [Fagotto et al., 1994] for $M = 0.5M_\odot$, $Z = 0.05$, $Y = 0.35$ is shown as the thin line marked as "F1994". It means that low mass PNN and WD are at the edge inside the SD domain and, hence, sometimes they may be confused with SD. The grey ellipse shows the domain of the SDs after evolution in close binaries [Han et al., 2003]. It expands the SD domain considerably: apparently SD may be almost anywhere on the "lg T_{eff} – lg L" plane between the solar ZAMS and the classic PNN-WD track (2 thick lines in the Fig. 1). But single (and without a binary past) very hot SDs have not been explained by known evolutionary tracks.

Two SD domains are seen *from the models* fainter and hotter than the solar ZAMS:

evolved SDs with $4.05 < \lg\ T_{eff} < 4.8$ ($11000 < T_{eff} < 60000$ K, spectral classes sdO and sdB, $(J-Ks) < 0$, $0 < \lg\ L < 3$, $2 < M_{Ks} < 8$, hereafter ESDs),

unevolved SDs with $\lg\ T_{eff} < 3.85$ ($T_{eff} < 7000$ K, spectral classes sdF and later, $(J-Ks) > 0.1$, $\lg\ L < 0.5$, $M_{Ks} > 2$, hereafter USDs).

The gap between these domains should not be populated by single USDs because they would have low metallicity but been born within the last 7 Gyr. However, some binaries of a ESD and a redder dwarf must have $(J-Ks) > 0$ and fill the gap. Real data should be used to test it.

To be rather numerous in the large surveys the SDs 1) stay in the domain for a long time: several Gyr for USD and about 100 Myr for ESD, 2) deviate considerably from the solar ZAMS (the data used must be quite precise).

The USDs look as a quite homogeneous population: low-metallicity population II stars with little or no galactic rotation. By definition they are at a low-metallicity ZAMS. Therefore, their distribution on mass and age is determined by yet poorly known birthrate. For example, if all low-metallicity stars were born only more than 7 Gyr ago then all USDs have masses $M < 0.9M_\odot$ (more massive SDs have leaved ZAMS) and, hence, T_{eff}, spectra and $(J-Ks)$ are as pointed out early. However, if some low-metallicity stars were born within the last 7 Gyr in a satellite merged by the Galaxy then one could find more massive, hot and bright USD.

In contrast to USDs the ESDs is a heterogeneous population. The only common feature for ESDs is the mass nearly 0.4-0.6$M_\odot$ because no a theoretical track of a more massive star in the ESD domain but less massive ones are not so evolved. Many of ESDs are helium rich and the most of them are helium core burning stars with extremely thin hydrogen envelops (the extended horizontal branch (EHB) stars). The tracks in Fig. 1 show that ESDs have various metallicities: very low, nearly solar, very high and even unusual ones with low Z and high Y.

Moreover, ESDs look even more complex when one takes into the account other ways putting the evolved stars to the ESD domain. The reason of this diversity of ESDs is that the usual evolutionary way from the RGB through horizontal branch (HB), asymptotic giant

branch (AGB), PNN to WD sequence can be deviated or interrupted to put a star into the ESD domain. Since new evolutionary ways to ESD could be found in the future, we discuss the known ones only briefly. Various scenarios of the mass loss at the RGB and helium flash at the RGB tip, as well as the evolution of close binaries are most important because future ESD has to be quite massive before the helium flash to rich it for a reasonable time yet much less massive to enter the ESD domain. A star becomes a ESD coming from RGB tip [Catelan, 2007], EHB [Fagotto et al., 1994], the early-AGB and AGB similar to PNN-WD way but inside the ESD domain [Fagotto et al., 1994], [Catelan, 2007], WD (hot-flasher scenario with helium flash delay by [Miller Bertolami et al., 2008]), a pair of merging WDs or evolution of binary [Han et al., 2003], and probably some other exotic ways. Thus, the ESDs can have various ages, metallicities as well as various velocities with respect to the galactic centre which is known as the asymmetric drift of the different populations at the solar distance from the centre.

3 The data

The Tycho-2 B_T, V_T photometry and proper motions are used when the precision is better than 0.2^m and 7 milliarcsec year^{-1} (hereafter mas yr^{-1}) respectively.

The XPM catalogue is made in Kharkov National University, Ukraine. It combines the positions from the 2MASS and USNO-A2.0 [Monet, 1998] catalogues in order to derive the absolute proper motions of about 280 million stars distributed all over the sky excluding a small region near the Galactic Centre, in the magnitude range $12^m < B < 19^m$. The mean epoch difference of the positions used is about of 45 years for the Northern hemisphere and 17 years for the Southern one. The zero-point of the absolute proper motion frame (the "absolute calibration") was specified with the use of about 1.45 million galaxies from the 2MASS. Most of the systematic zonal errors inherent in the USNO-A2.0 catalogue were eliminated before the calculation of proper motions. The mean formal error of absolute calibration is less than 1 mas yr^{-1} [Fedorov, Myznikov & Akhmetov, 2009].

The third U.S. Naval Observatory CCD Astrograph Catalog, UCAC3 is a compiled, all-sky star catalogue covering mainly the 8 to 16 magnitude range in a single bandpass between V and R. We use its proper motions and photometry. The latter are UCAC3 own band photometry (hereafter R_{UCAC3}), 3 bands of 2MASS (J, H, Ks) and 3 bands from the SuperCosmos project [Hambly, Irwin & MacGillivray, 2001] (hereafter B_{SC}, R_{SC}, I_{SC}). The proper motions of bright stars are based on about 140 catalogs, including Hipparcos [Hipparcos and Tycho catalogues, 1997], Tycho and all catalogs used for the Tycho-2 proper motion construction. Proper motions of faint stars are based on a re-reduction of early epoch SPM data (δ from $-90°$ to $-10°$) plus Schmidt plate data from the SuperCosmos project (down weighted due to systematic errors of order 0.1 arcsec). The proper motions of faint stars (R_{UCAC3} $\geq$13.5) therefore should be used with caution [Zacharias et al., 2009]. The unpublished plate measure data from the several astrometric catalogues have considerably contributed to improve proper motions for stars mainly in the 10 to 14 mag range (the interval which is most interesting for us); however, these data do not cover all sky as pointed out by [Zacharias et al., 2009].

As pointed out early, precise IR photometry is the key data for our study. Therefore, we consider only stars with $6 < Ks < 14$ following the error budget of the 2MASS photometry. The UCAC3 and SuperCosmos photometry cover all this photometric interval but

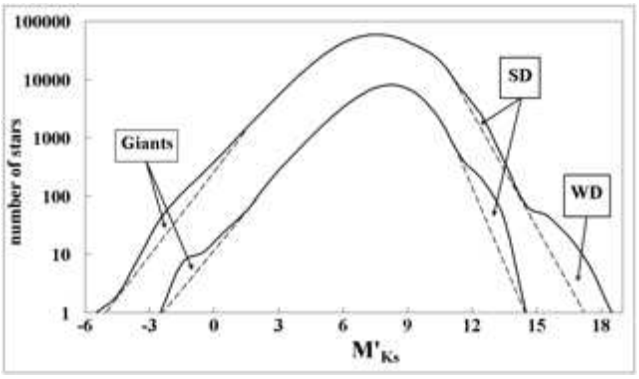

Figure 2: The distribution of the XPM stars along M'_{Ks} for $0.34 < (J - Ks) < 0.35$ The higher thick curve is for $|b| < 10°$, the lower thick one is for $|b| > 50°$. The deviations of these curves from the dashed lines are giants, SDs and WDs.

not for all stars. The R_{UCAC3} accuracy is believed to be at the level of 0.1-0.2 mag whereas SuperCosmos typical photometric accuracy is about of 0.3 mag. However, as declared by [Hambly, Irwin & MacGillivray, 2001], the $B_{SC} - R_{SC}$ and $R_{SC} - I_{SC}$ colors are accurate to 0.07 mag.

There are about 47 millions stars with $Ks < 14$ common to the 2MASS, XPM and UCAC3. The mean difference of their proper motions in the sense "UCAC3 minus XPM" is quite small: $\overline{\Delta\mu_\alpha \cos(\delta)} = -2.8$ mas yr^{-1}, $\overline{\Delta\mu_\delta} = +0.3$ mas yr^{-1}. The standard deviations of their proper motion differences are $\sigma(\Delta\mu_\alpha \cos(\delta)) = 12$ mas yr^{-1}, $\sigma(\Delta\mu_\delta) = 12$ mas yr^{-1}. Taking into the account that majority of the common stars has $Ks \approx 14$ their accuracy of the UCAC3 proper motion components is near 6-8 mas yr^{-1} as declared for faint stars by [Zacharias et al., 2009]. Consequently, we conclude that the XPM proper motion accuracy has nearly the same level. The detail comparison of the XPM and UCAC3 as well as analysis of the XPM proper motion errors are presented elsewhere [Fedorov et al., 2010].

The proper motion difference "UCAC3 minus XPM" seems not to depend on XPM epoch difference or another parameter. Therefore, we simply select for the investigation about 23.4 million stars with good precision of the UCAC3 proper motions and good agreement of them with the ones from the XPM (in mas yr^{-1}):

$$\Delta\mu_\alpha \cos(\delta) < 10 \ , \ \Delta\mu_\delta < 10 \ , \ \sigma(\mu_{UCAC3}) < 15 \qquad (4)$$

The means of the UCAC3 and XPM proper motions of the stars are used hereafter, except Tycho-2 stars among them for which the Hipparcos or Tycho-2 proper motions are used depending on their formal errors.

4 Selection of the stars

In contrast to simple selections of SDs in the "$(J - Ks)$ – M'_{Ks}" plane (for example, by [Smith et al., 2009]) we fulfill the detailed analysis of the distribution of Tycho-2, XPM and UCAC3 SDs and WDs for the whole interval of $(J - Ks)$, M'_{Ks} and all latitudes as well as pay special attention to the estimation of admixtures in the samples. In addition we analyze the distribution of stars in the "$(B_T - V_T)$ – M'_{V_T}" and "$(B_{SC} - I_{SC})$ – $M'_{B_{SC}}$" planes to eliminate erroneous classifications due to duplicity (see later).

Firstly, the distribution of the stars in the "$(J-Ks)$ – M'_{Ks}" plane is approximated by 4 Gaussians corresponding to giants, main sequence (MS) stars, SDs and WDs. Then the MS-SD and SD-WD cut lines are found between the Gaussians as some polynomial functions of $(J-Ks)$ in order to make the samples containing no more than 10% of admixture stars. An example of the distribution of the XPM stars along M'_{Ks} for $0.34 < (J-Ks) < 0.35$ (a section of 4 Gaussians) is presented in Fig. 2. The higher thick curve is for $|b| < 10°$, where b is the galactic latitude. The lower thick curve is for $|b| > 50°$. The deviations of these curves from the dashed lines are due to heterogeneous distribution of stars on velocity (with respect to the Sun) and, hence, correspond to non-MS stars, namely, giants, SDs and WDs. For $0.34 < (J-Ks) < 0.35$ the SDs should be selected at $12.25 < M'_{Ks} < 15$ and WDs at $M'_{Ks} > 15$.

It is found that

- the distribution of Tycho-2 stars is strongly affected by the magnitude limit of the catalogue about $V_T \approx 11$ mag and, hence, it contains few WDs and USDs; therefore, the cut lines in the "$(J-Ks)$ – M'_{Ks}" plane are taken from XPM and UCAC3 only,
- the SD-WD cut line is affected by the magnitude limits of the XPM and UCAC3 providing variations of SD admixture in the WD sample for $M'_{Ks} \geq 15$, therefore, this cut line is not so well determined as the MS-SD one,
- SDs at different b cover the same interval of M'_{Ks} (as seen in Fig. 2) and, hence, the cut lines do not depend on b,
- the distributions for UCAC3 and XPM are fairly the same that proves the same level of accuracy of these catalogues,
- WDs are noticeable only at low latitudes.

The final MS-SD cut line giving the SD sample with less than 10% admixture is

$$M'_{Ks} > 11.766(J-Ks)^3 - 16.804(J-Ks)^2 + 12.365(J-Ks) + 9.5 \quad (5)$$

It is found that the SD-WD cut line has sense only for $-0.1 < (J-Ks) < 0.7$ and for some latitudes. Star should be a WD if

$$M'_{Ks} > -13.036(J-Ks)^2 + 11.585(J-Ks) + 12.65 \quad (6)$$

A Monte-Carlo simulation similar to GG2009 is made to test the empirically obtained cut lines. The content of 2MASS catalogue for MS, ESD, USD and WD stars is reproduced to analyze their distribution in the "$(J-Ks)$ – M'_{Ks}" plane. The photometric and astrometric errors with realistic dispersions are applied.

We used normal and uniform distributions realized with the Microsoft Excel 2007 random number generator, whose general description was given by [Wichman & Hill, 1982]. We consider 4 categories of stars: MS, ESD, USD and WD. For each category we generated 200000 model stars with specified

- the uniform distributions in rectangular galactic X and Y coordinates and distribution in Z following [Robin et al., 2003] and [Veltz et al., 2008],

- the distributions in velocity components along the galactic longitude l and latitude b, V_l, and V_b following [Robin et al., 2003] and [Veltz et al., 2008],
- the distributions in $(J-Ks)$, the dependence of M_{Ks} on $(J-Ks)$ and its scatter following [Girardi et al., 2000] and [Girardi et al., 2005] and variations of the distribution of the stars on the metallicity,
- the interstellar extinction A_{Ks} calculated as $0.11A_V$ where A_V is calculated following new model of extinction by [Gontcharov, 2009b] taking into the account the extinction in the Gould belt,
- the errors of 2MASS photometry for $Ks < 14$ accepted as 0.05 mag and errors of proper motions widely varied.

Then for every model star we calculate

- true distance $R = (X^2 + Y^2 + Z^2)^{1/2}$,
- l and b: $\tan(l) = Y/X$, $\tan(b) = Z/(X^2 + Y^2)^{1/2}$,
- $\mu_l = V_l/(4.74R)$, $\mu_b = V_b/(4.74R)$,
- total proper motion $\mu = (\mu_l^2 + \mu_b^2)^{1/2}$,
- $Ks = M_{Ks} - 5 + 5\lg(R) + A_{Ks}$,
- truncation of the sample by $Ks < 14$,
- M'_{Ks} from Ks, μ and A_{Ks} following the equation 1.

The simulation proves that the input dispersions (including errors) translate into the output dispersion of the stellar distribution on M'_{Ks} so that

- the photometric errors at the level of 0.05 mag or lower do not influence the output dispersions,
- the reasonable variations of the metallicity distribution do not influence the output dispersions,
- the proper motion errors are very important: the MS output dispersion rises with it so that *pure and complete* SD and WD samples for $(J-Ks) < 0.7$ could be obtained when the proper motion error is at the level of 1 mas yr^{-1} whereas no SD or WD sample could be obtained when the error is at the level of 20 mas yr^{-1}, the level of the typical proper motion itself,
- the obtained cut lines are correct to make 90%-clear SD sample if the proper motion mean error is about of 10 mas yr^{-1}, but it gives strong biases because many slow stars are lost,
- no MS-SD-WD separation for $(J-Ks) > 0.7$ (only $(J-Ks) < 0.7$ are considered later).

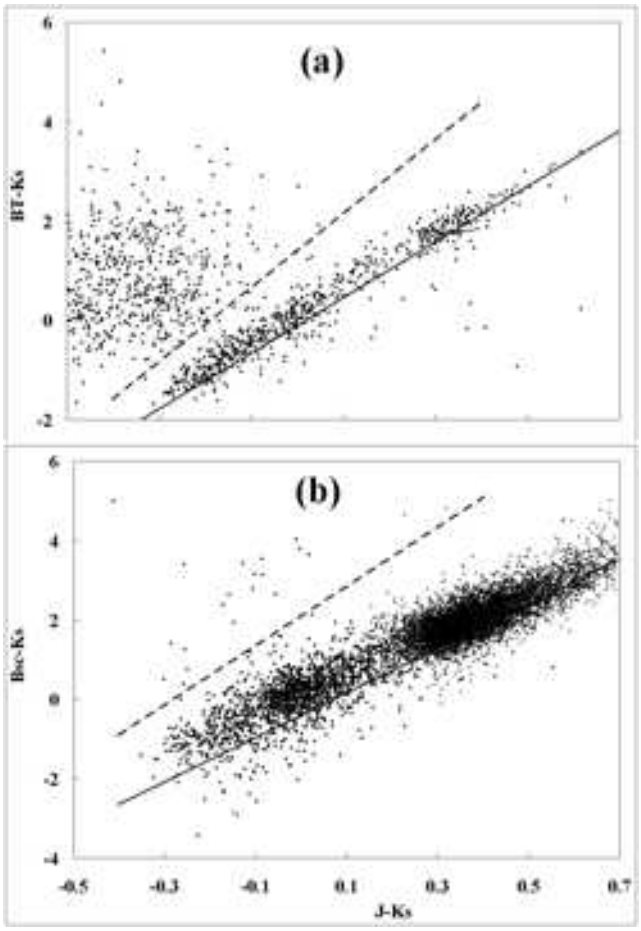

Figure 3: The stars selected by use of the equation 5: (a) Tycho-2 stars in the diagram "$(J-Ks)$ vs. (B_T-Ks)", (b) XPM-UCAC3 ones in the diagram "$(J-Ks)$ vs. $(B_{SC}-Ks)$". The empirical ZAMS are shown by solid lines. The dashed lines show the theoretical reddening slope and separate the stars with normal color relations from the ones with color discrepancies.

- the reddening because of extinction strongly affects the selection of ESDs: the stars with large reddening are lost but the rest stars have negligible extinction,
- as expected after GG2009, the purity, completeness in some region of space, and symmetry (in favor to slow or fast stars) cannot be combined in the same sample, and we prefer the purity accepting such cut lines.

The stars selected by use of the equation 5 are shown in Fig. 3: (a) Tycho-2 stars in the diagram "$(J-Ks)$ vs. (B_T-Ks)" and (b) rest stars in the diagram "$(J-Ks)$ vs. $(B_{SC}-Ks)$". The empirical ZAMS $(B_T-Ks)=5.6(J-Ks)-0.1$ and the line $(B_T-Ks)=7.5(J-Ks)+1.4$ with theoretical reddening slope both taken from [Gontcharov, 2008a] are shown in Fig. 3 (a) for Tycho-2 stars by thick and dashed lines respectively. Similar lines shifted due to B_T-B_{SC} difference are shown in Fig. 3 (b) for rest stars: $(B_{SC}-Ks)=5.6(J-Ks)-0.4$ and $(B_{SC}-Ks)=7.5(J-Ks)+2.1$. The spread of the dots near the ZAMS is due to the photometric errors and reddening shift. The stars lower than the ZAMS are prove to be binaries with composite spectrum [Stark & Wade, 2003]. The stars higher

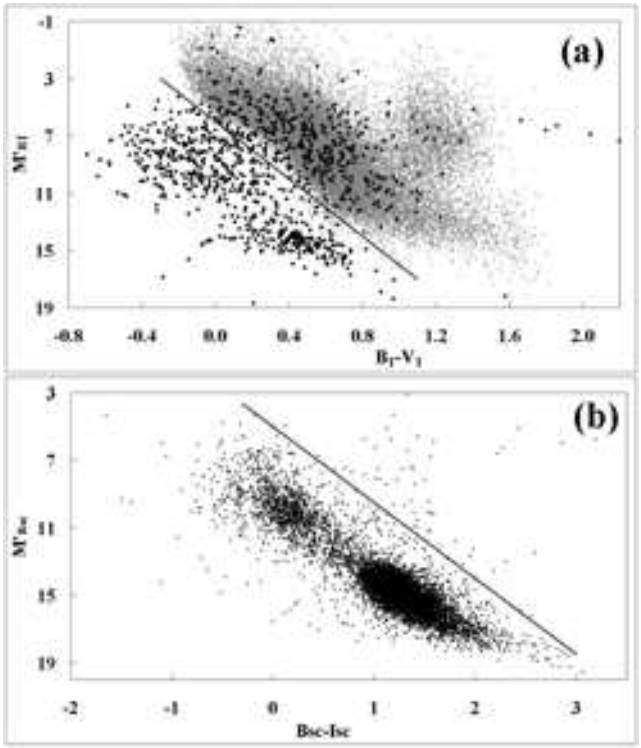

Figure 4: The stars selected by use of the equation 5: (a) Tycho-2 stars in the diagram "$(B_T - V_T)$ – M'_{V_T}", (b) XPM-UCAC3 ones in the diagram "$(B_{SC} - I_{SC})$ – $M'_{B_{SC}}$". The lines separate the suspected SDs and WDs from the rest stars.

than the reddening lines show the discrepancy between their colors. It can be explain by stellar duplicity, known in most cases or hidden. It gives visual-IR identification mistakes and/or unusual energy distribution in the common spectrum. However, one should not simply eliminate these stars because some of them could contain SD or WD components, specially, taking into account that the binary fraction in ESD stars is much higher than for normal stars [Østensen, 2009].

The pairs with subluminous components can be separated from the rest binaries in the diagrams "$(B_T - V_T)$ – M'_{V_T}" and "$(B_{SC} - I_{SC})$ – $M'_{B_{SC}}$" after the main selection by use of the equation 5. These two diagrams for stars selected by use of the equation 5 are shown in Fig. 4 (a) and (b) respectively. In fact, the former diagram contains Tycho-2 stars and the latter one does the rest stars. The Hipparcos stars [van Leeuwen, 2007] with parallax relative error less than 0.3 are shown in the former diagram as the grey "cloud" of points. It could not be provided for the latter diagram because no precise B_{SC} and I_{SC} for the Hipparcos stars. The cut lines are shown: $M'_{V_T} = 10(B_T - V_T) + 6$ and $M'_{B_{SC}} = 4.5(B_{SC} - I_{SC}) + 5$. All stars higher than the lines are eliminated. The plane "$(J - Ks)$ – M'_{Ks}" is preferred for main selection because the $(J - Ks)$ for the stars is much more precise than the $(B_T - V_T)$ or $(B_{SC} - I_{SC})$.

The final sample of 9799 SD and WD candidates is shown in Fig. 5. in the diagram "$(J - Ks)$ – M'_{Ks}" together with the Hipparcos stars with parallax relative error less than 0.3 (the grey "cloud" of points). The 1040 stars selected from Tycho-2 are shown in subfigure (a) whereas 8759 ones from XPM and UCAC3 are in subfigure (b) (358 Tycho-2 stars are

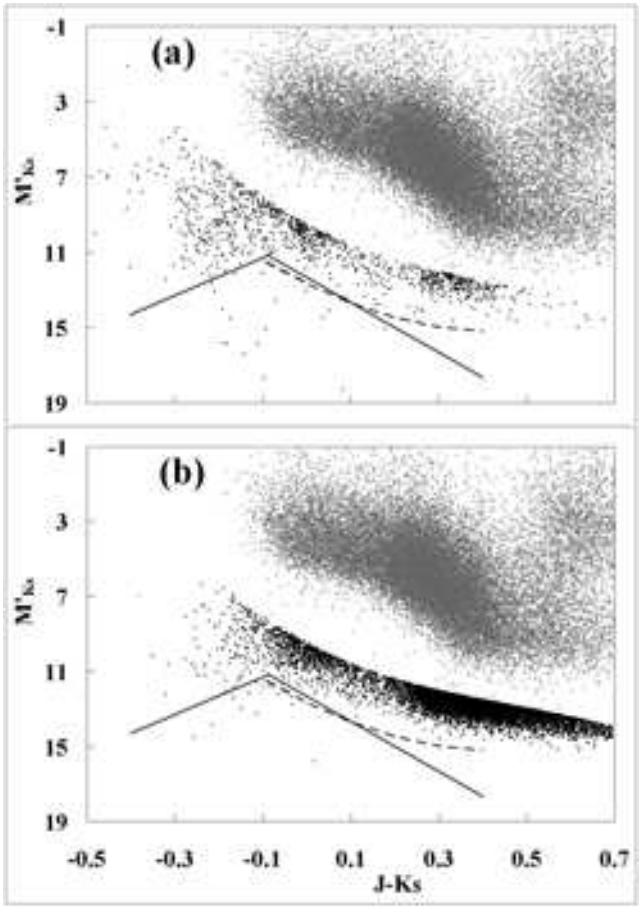

Figure 5: Hipparcos stars with parallax relative error less than 0.3 (grey points) together with selected (a) 1040 Tycho-2 and (b) 8759 XPM-UCAC3 stars (black diamonds), SD-WD cut from equation 6 (dashed line) and accepted SD-WD cut (thick polygonal line).

also XPM and UCAC3 ones but their Tycho-2 proper motions are preferred). The MS-SD cut line is evident as the higher border of the black bulk. The SD-WD cut line from the equation 6 is shown as dashed line. But it is obtained only for $(J-Ks) > -0.1$ and no WD found for $(J-Ks) > 0.2$. Therefore, for the selection of WDs we accept the polygonal thick line shown in the Fig. 5:

$$M'_{Ks} > 10.3 - 10(J-Ks), \qquad if (J-Ks) < -0.09;$$
$$M'_{Ks} > 12.3 + 13.3(J-Ks), \qquad if (J-Ks) \geq -0.09. \tag{7}$$

Since this SD-WD separation is a matter of convention, some our SDs with $(J-Ks) < -0.1$ may be WDs and vice versa.

The gap between the grey and black bulks means that we have to apply rather strong cut to get rather pure sample. Therefore, we expect to lose many or even majority of slow SDs and some known ones selected by spectroscopy. However, the obtained large samples of stars with high probability to be SDs or WDs seems to be useful not only for current study of their properties but for the next spectroscopic studies.

Two domains, the ESDs and USDs are evident near $(J-Ks) \approx 0$ and $\approx 0.3-0.4$ respectively. As expected the USDs are much more numerous than ESDs. But Tycho-2

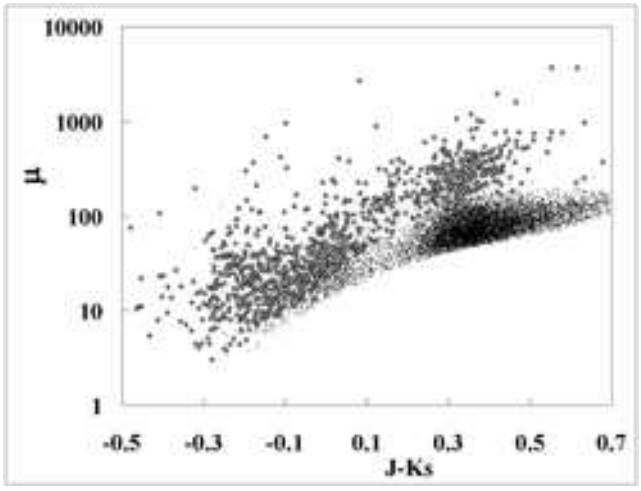

Figure 6: The distribution of the Tycho-2 (open diamonds) and XPM-UCAC3 (crosses) selected stars in the diagram "$(J-Ks)$ vs. total proper motion (in mas yr^{-1})".

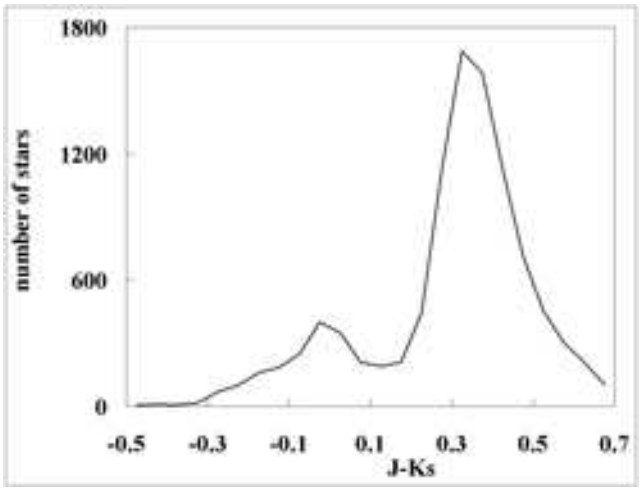

Figure 7: The distribution of the selected stars on $(J-Ks)$.

contains too little USDs because of the magnitude limitation.

The distribution of the Tycho-2 (open diamonds) and XPM-UCAC3 (crosses) selected stars in the diagram "$(J-Ks)$ vs. total proper motion" is shown in Fig. 6. The proper motions are in mas yr^{-1}. The both subsamples show ESD and USD overdensities at the same $(J-Ks)$.

The distribution of the selected stars on $(J-Ks)$ is shown in Fig. 7. The ESD and USD Gaussians are evident here with some asymmetries due to binaries and reddening.

The number of selected stars by band, magnitude range, median magnitude and median photometric error are presented in Table 1.

The ESDs and WDs are separated from the USDs in some color-color diagrams: examples of these separated overdensities are presented in Fig. 8. The reddest overdensities are USDs, the middle and the bluest ones are ESDs with some admixture of WDs and unevenly distributed ESD binaries. The separation of the USDs from the rest stars is explained by some

Table 1: Number of selected stars by band, magnitude range, median magnitude and median photometric error.

	stars	mag range	median mag	median error
B_T	737	7.6-13.1	11.9	0.10
V_T	648	7.3-12.8	11.7	0.13
B_{SC}	8961	8.9-18.4	15.3	≈0.2
R_{SC}	9113	9.0-16.9	14.6	≈0.2
I_{SC}	9113	9.3-16.8	14.1	≈0.2
R_{UCAC3}	7434	9.4-17.3	15.0	0.13
J	9799	6.7-14.7	13.8	0.03
Ks	9799	6.5-14.0	13.5	0.03

differences in their spectra. It allows us to separate the USDs with some level of probability by use of all the following empirical conditions:

$$\begin{gathered}(J-Ks)>0.06\\(B_{SC}-I_{SC})>0.75\\(B_{SC}-R_{SC})>0.42\\(R_{UCAC3}-Ks)>1.25\\(B_{SC}-Ks)>1.8-(R_{UCAC3}-R_{SC})\\(J-Ks)>0.15,\end{gathered} \tag{8}$$

The formula 7 and 4 are used to separate 3 subsamples among the 9799 selected stars: 7769 USDs, 1996 ESDs and 34 WDs.

5 Statistics of the selected stars

The distribution of the selected stars on J magnitude is shown in Fig. 9: dashed-dotted line for WDs, dotted one for ESDs, dashed one for USDs and solid line for total distribution. Some overdensities at $J \approx 7^m$, $\approx 10.5^m$ and $\approx 13.5^m$ are related to the maxima in the Hipparcos, Tycho-2 and 2MASS distribution respectively. It means that the selection criteria are stronger for fainter stars. Consequently, the completeness decreases with magnitude and distance so that the ESD and USD samples are almost complete to $J \approx 8^m$ or distance $R \approx 60$ pc and substantially ($\approx 70\%$) complete to $J \approx 10.5^m$ or distance $R \approx 200$ pc.

Hipparos contains 153 selected stars. There is spectral classification for 140 stars from Tycho Spectral Types catalog (TST) by [Wright et al., 2003] or other sources. In many cases the classification is marked as doubtful. Only 27 stars are classified as SDs and 10 as WDs.

The Fig. 10 presents the Hipparcos stars with parallax relative error less than 0.3 in the diagram "$(J-Ks)$ vs. M_{Ks}" where M_{Ks} is calculated from the Hipparcos parallaxes: all stars (grey "cloud" of points), selected ESDs (black and open bold circles), selected WDs (black and open bold diamonds), selected USDs (black and open bold squares), the same categories with spectroscopic classification from the TST and other sources (the same but open light and open bold signs). In the figure the open signs of classified stars are drawn over black ones of the selected stars. Therefore, finally the black signs are the selected stars

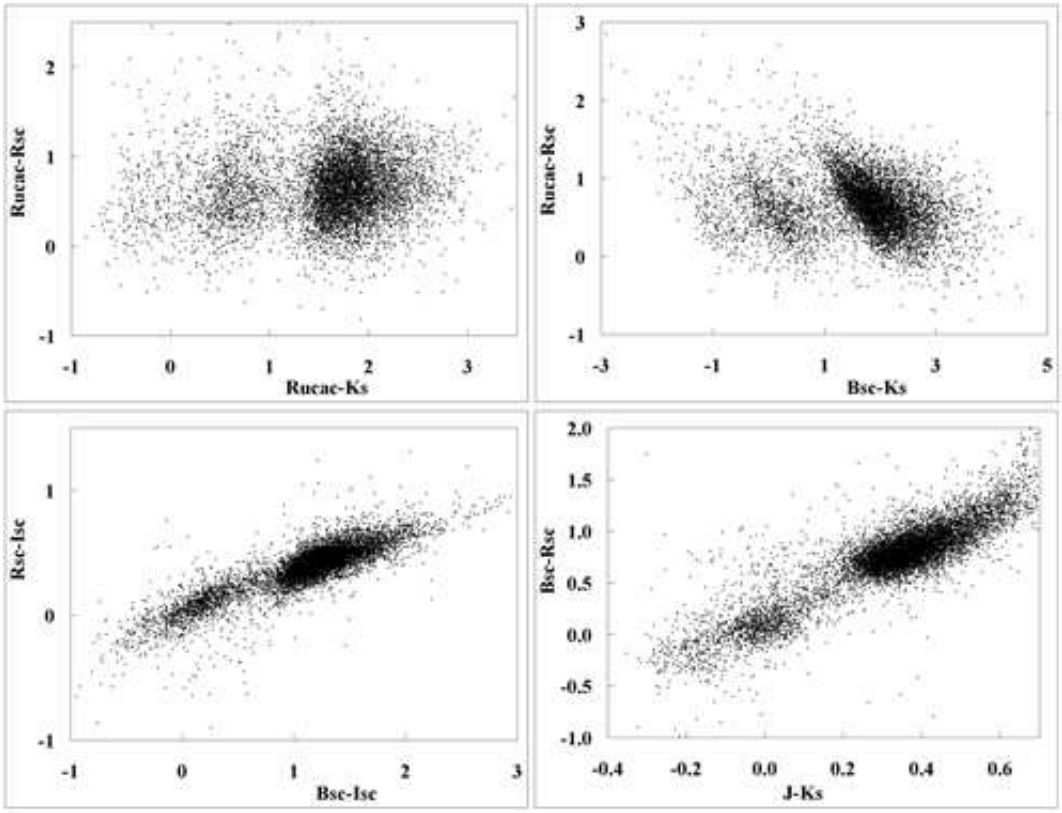

Figure 8: Some color-color diagrams to separate USDs form the rest stars.

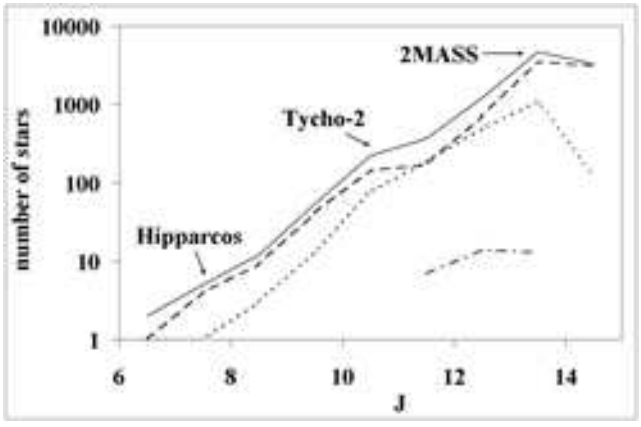

Figure 9: The distribution of the selected stars on J magnitude: dashed-dotted line for WDs, dotted one for ESDs, dashed one for USDs and solid line for total distribution. Some overdensities due to catalogue maxima are marked.

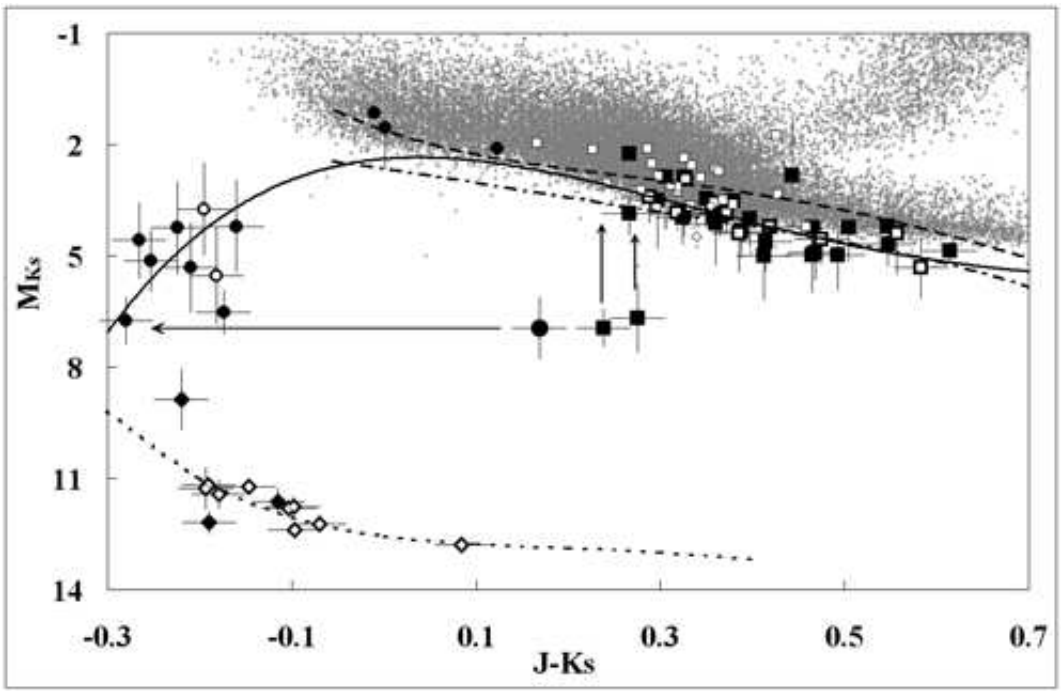

Figure 10: Hipparcos stars with parallax relative error less than 0.3 in the diagram "$(J-Ks)$ vs. M_{Ks}": all stars (grey "cloud" of points), selected ESDs (black and open bold circles), selected WDs (black and open bold diamonds), selected USDs (black and open bold squares), the same categories with spectroscopic classification from the TST and other sources (the same but bold and light open signs). The dash-dotted and dashed lines show the isochrones for metallicities $Z = 0.001$ and $Z = 0.019$. The accepted calibrations are shown for SDs (solid line) and WDs (dotted line). The arrows show suspected replacement of 3 discussed outliers.

without right spectral classification, the open bold signs are the cases when our identification fits spectral classification (2 ESDs, 9 WDs and 10 USDs) and the light open signs are the stars which are classified but not selected (1 ESD, 3 WDs and 23 USDs). It is evident from the absolute magnitudes that the ESD and WDs which are classified but not selected have wrong spectral classification. Perhaps, the same is right for some of the classified but not selected USDs. Thus, the mistakes in spectral classification of the subluminous stars are common. Our method helps to verify the status of the stars. The comparison of the fainter (non-Hipparcos) stars of our samples with the known lists of classified subluminous stars will be provided elsewhere.

Three selected stars with $0.1 < (J-Ks) < 0.3$ and $M_{Ks} \approx 7$ are interesting examples of the complexity of correct selection of subluminous stars. They are HIP 47296, 10529 and 3446. HIP 47296 has been classified by spectrum as a suspected white dwarf. Its "$(J-Ks)$ – $(B_T - V_T)$" relation proposes duplicity and composite spectrum. Probably its duplicity also effects parallax giving its large error of 3 mas. But no way to fit the parallax and M_{Ks} for a WD. $(B_T - V_T) = -0.53$ in combination with $M_{Ks} = 7$ suspects a SD component instead of WD. For this star we accept the Hipparcos M_{Ks} instead of the calibrated one. HIP 10529 is a known pair with HIP 10531, probably optical. Its parallax may be wrong. The colors are agreed, therefore, it must be a USD. HIP 3446 has large error of the parallax (3 mas) and a discrepancy of the colors. It must mean duplicity with a component to be a USD. The arrows in Fig. 10 show the suspected replacement of these 3 outliers to their real positions in the plane. We conclude that duplicity is very important for the treatment of the subluminous stars.

The lines in the Fig. 10 are related to the "$(J-Ks)$ vs. M_{Ks}" calibration. The dotted line shows the accepted empirical calibration for WDs close to the theoretical calibration for the TRILEGAL code by [Girardi et al., 2005]:

$$M_{Ks} = -23.364(J-Ks)^4 + 33.36(J-Ks)^3 - 14.051(J-Ks)^2 + 3.346(J-Ks) + 12.53 \quad (8)$$

Its accuracy due to intrinsic spread of the data is 0.2^m.

The dash-dotted and dashed lines show the isochrones for metallicities $Z = 0.001$ (typical for thick disk and halo) and $Z = 0.019$ (solar one) respectively [Girardi et al., 2000]. The former fits redder USDs whereas the latter does bluer ones and some ESDs. Generally it fits the suspects about their metallicities and ages. The solid line is the accepted polynomial calibration

$$M_{Ks} = 18.28(J-Ks)^4 - 42.968(J-Ks)^3 + 30.359(J-Ks)^2 - 2.1323(J-Ks) + 2.38 \quad (9)$$

Its intrinsic spread is about 0.3^m for USDs and about 1^m for ESDs. In fact it reflects the homo/heterogeneous nature of the subsamples.

It has been shown that the $(J-Ks)$ for some binaries can be erroneous. Therefore, for all the selected stars with color index discrepancies the empirical calibration is used:

$$M_{Ks} = 0.5442 M'_{Ks} - 0.876 \quad (10)$$

The accuracy of this calibration is estimated from the spread of the Hipparcos stars with well-known parallaxes as about 1^m.

Photoastrometric (R_{RPM}, in cases of color index discrepancies) and photometric (R_{ph}, in rest cases) distances as well as related rectangular coordinates XYZ are calculated for the selected stars by use of the calibrated M_{Ks} from $\lg(R_{ph}) = (Ks - M_{Ks} + 5 - A_{Ks})/5$ (for the

sake of simplicity all the obtained distances are referred as R_{ph} hereafter). The interstellar extinction A_{Ks} generally no more than 0.2^m for the $R < 2$ kpc and, hence, lower than the errors of the photometry and calibration. Therefore, the extinction is ignored.

The relations between the obtained and Hipparcos values are shown in Fig. 11: (a) M_{Ks} vs. $M_{Ks}HIP$, (b) R_{ph} vs. R_{HIP} (in pc). The WDs, ESDs and USDs with precise parallaxes (relative error less than 0.3) are shown by diamonds, circles and squares respectively. Two mentioned binaries (HIP 10529 and 3446) are shown by open signs. Unfortunately, for ESDs the both distances, R_{ph} and R_{HIP} have low accuracy.

The distribution of all the selected stars on the celestial sphere in galactic coordinates is shown in Fig. 12: (a) ESDs, (b) USDs and (c) WDs. The same for the Tycho-2 selected stars is shown in Fig. 12 (d), (e), (f). It is seen that no WDs at high latitudes. The distribution of all USDs is strongly affected by the UCAC3 selection in favor to the southern equatorial hemisphere. The distributions of the ESDs and USDs show some voids at the galactic centre and along the Gould belt because of the extinction considered by [Gontcharov, 2009b]. Despite the voids both ESDs and USDs show considerable concentration to the galactic centre hemisphere.

Some overdensities of the ESDs are seen both among Tycho-2 and UCAC3-XPM stars at:

1. $l \approx 218$, $b \approx +5$,
2. $l \approx 278$, $b \approx -32$, in front of the LMC,
3. $l \approx 287$, $b \approx -2$, at $\eta\ Car$ region,
4. $l \approx 314$, $b \approx +15$, at Sco-Cen association,
5. $l \approx 318$, $b \approx -12$,
6. $l \approx 332$, $b \approx -2$,
7. $l \approx 5$, $b \approx -42$,
8. $l \approx 22$, $b \approx -32$,
9. $l \approx 33$, $b \approx -41$,
10. $l \approx 94$, $b \approx -2$,
11. $l \approx 137$, $b \approx -22$

A detail investigation of individual stars in the overdensities shows that they must be real. The nature of the overdensities is to be revealed. One may suspect them as some remnants of dwarf galaxies or globular clusters. Else, since some of the overdensities are near star formation regions, one could suspect an intense mass loss for the stars near the regions making so many ESDs.

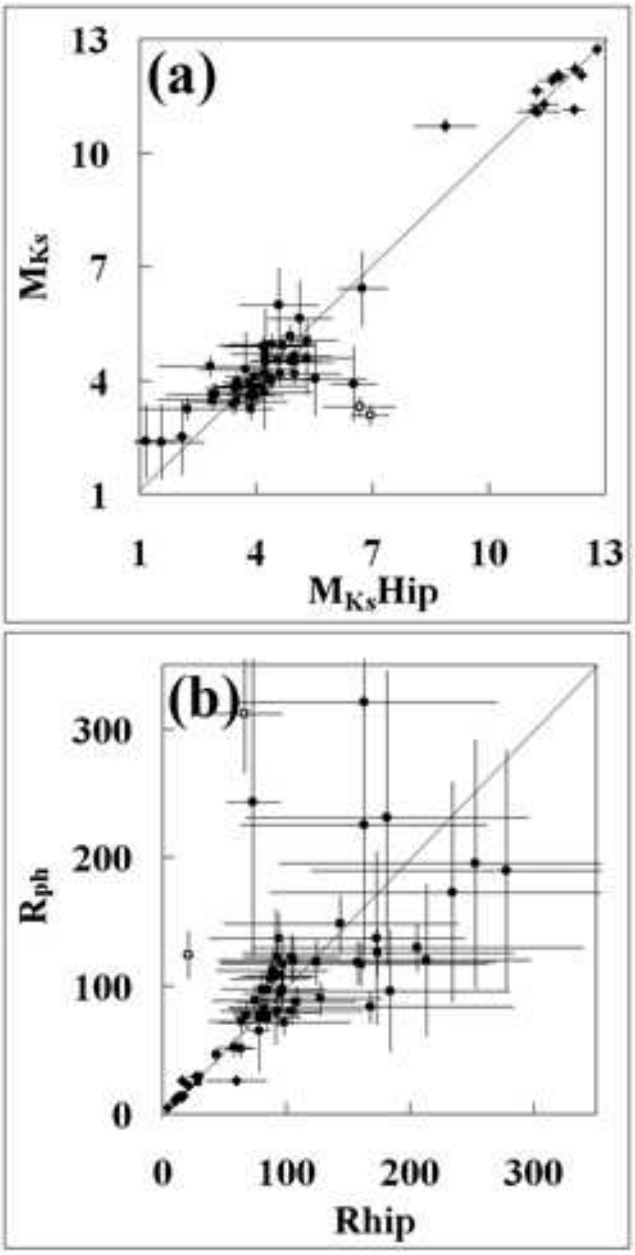

Figure 11: The relations (a) M_{Ks} vs. $M_{Ks}Hip$ and (b) R_{ph} vs. R_{HIP} (in pc) for WDs (diamonds), ESDs (circles) and USDs (squares) with precise parallaxes. The mentioned binaries are open signs.

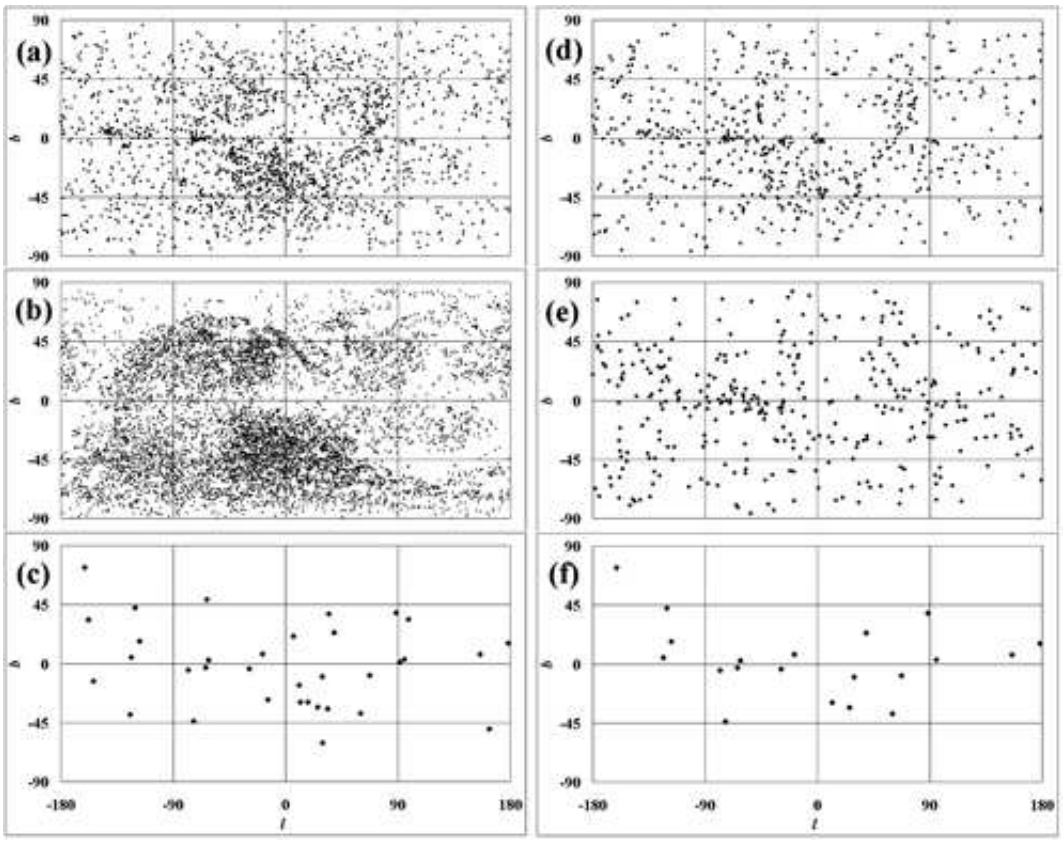

Figure 12: The distribution of all selected stars on the celestial sphere in galactic coordinates: (a) ESDs, (b) USDs and (c) WDs and the same for the Tycho-2 selected stars: (d), (e), (f).

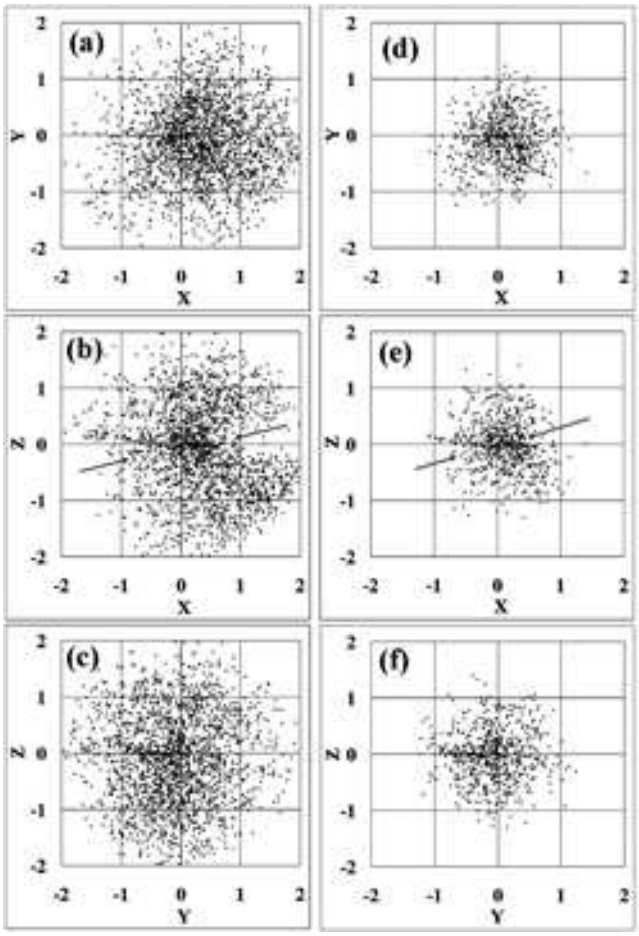

Figure 13: The distribution of all selected ESDs projected into the (a) XY, (b) XZ and (c) YZ planes as well as Tycho-2 ESDs projected into the same planes in (d), (e) and (f) subfigures (the distances in kpc).

6 3D distribution and motion of the stars

The distribution of the selected ESDs is shown in Fig. 13: all ESDs projected into the (a) XY, (b) XZ and (c) YZ planes as well as Tycho-2 ESDs projected into the same planes in (d), (e) and (f) subfigures (the distances in kpc). The same data for USDs are shown in Fig. 14. The distribution of the selected WDs is not shown because all of them are within 50 pc. The voids by the extinction near the galactic plane and in the Gould belt are evident in Fig. 14 for all subsamples quite dense at least to 500 pc. The Gould belt voids are marked by arrows in some XZ subfigures. Higher stellar density in the galactic centre hemisphere is evident. It gives new constraints to galactic models and will be analyzed in detail in next papers.

The Pulkovo Compilation of Radial Velocities (PCRV) catalogue [Gontcharov, 2006] contains radial velocities (RVs) for 78 selected stars with precision better than 5 km s^{-1}. Less precise RVs are collected from other sources for more 105 selected stars. Precise RVs are the crucial data for modern kinematic analysis of any stellar sample. Some advances in RV data are expected in near future. Therefore, in this *preliminary* study of the sample kinematics we use either 78 best RVs or all 183 RVs.

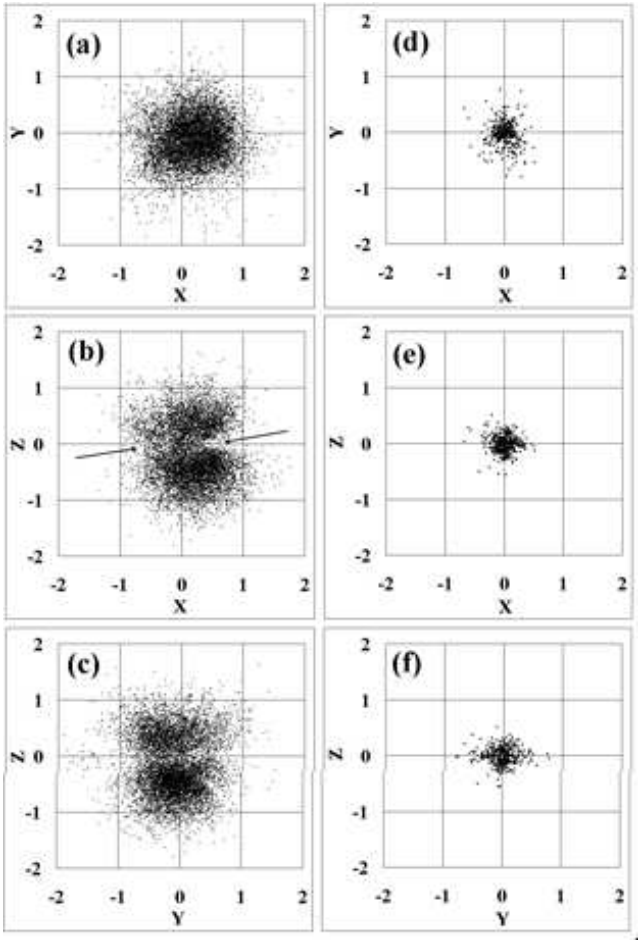

Figure 14: The distribution of all selected USDs projected into the (a) XY, (b) XZ and (c) YZ planes as well as Tycho-2 USDs projected into the same planes in (d), (e) and (f) subfigures (the distances in kpc).

Table 2: The mean/dispersion for U, V and W velocity components for ESDs and USDs (in km s^{-1}).

	U	V	W
ESD	30/92	-124/113	5/69
USD	-23/189	-267/94	-27/110

These RVs are used together with α, δ, μ and π or R_{ph} to calculate rectangular components U, V, W of the stellar space motion with respect to the Sun. No correction for galactic rotation and solar motion to the apex applied.

The Hipparcos distances highly correlate with R_{ph} for 78 best stars. Therefore, the main features of the stellar distribution in the 6D space of XYZUVW is the same for the both sets based on Hipparcos distances or R_{ph}. Here we consider only XYZUVW based on R_{ph}.

The mean and dispersion for U, V and W velocity components for 11 ESDs and 66 USDs is presented in Table 2 (in km s^{-1}). The asymmetric drift (considerable negative $\overline{V}$) is evident for both ESDs and USDs. For USDs it is similar to the Besançon galactic model value for halo: -226 km s^{-1} [Robin et al., 2003]. For ESDs it is between the Besançon halo and thick disk (-53 km s^{-1}) values proving that the ESDs is a heterogeneous sample with disk and halo stars. The same conclusions follow from the dispersions: the USDs show the dispersions similar to Besançon halo (131, 106, 85 km s^{-1} for U, V, W) biased due to selection in favor to faster stars whereas the ESD dispersions fall between the Besançon halo and thick disk (67, 51, 42 km s^{-1} for U, V, W).

The distribution of 1 WD (diamond), 11 ESDs (circles) and 66 USDs (open squares) with precise RVs in the projection to the UV, UW and VW planes (velocities in km s^{-1}) is shown in Fig. 15. The dispersion of the velocities and asymmetric drift in the V component are clearly seen allowing kinematic classification of the stars. The WD and most ESDs certainly belong to the galactic thin or thick disk (population I). As expected, most USDs belong to the halo (population II). Some of the USDs have retrograde motion. However, the distribution of the USDs along U and V is not normal. It means a strong bias due to the selection in favor to the higher velocities with respect to the Sun (as mentioned above, many slow SDs are lost due to selection method).

Metallicities Fe/H are collected for 56 stars from various sources. The relation of the Fe/H and velocity component V is shown in Fig. 16 for ESDs (circles) and USDs (open squares). The error bars show the estimation of the accuracy of V from the ones of μ, RV and R_{ph} as well as the error of about 0.3 dex accepted for Fe/H. The solar position is marked. The vertical lines show the separation of thin/thick disk at about Fe/H≈ -0.3 (Z≈ 0.01) and thick disk/halo at about Fe/H≈ -1.3 (Z≈ 0.001) similar to [Robin et al., 2003]. The ESDs are found both in halo and disk. The thin-thick disk separation is not evident in these data. The USDs belong to halo and probably to thick disk (taking into account that the errors for the most metal rich USDs are at the halo/disk boundary). The velocity-metallicity trend is evident for the USDs. For the ESDs only 2 stars in the halo domain are velocity outliers. The rest ESDs show no trend. One of 2 high velocity low metallicity ESD outliers, HIP 103755 is known RR Lyr variable [Hipparcos and Tycho catalogues, 1997].

There is a relation between Fe/H of SD and its position in the "$(J-Ks)$ vs. M_{Ks}" diagram. The ESDs (circles) and USDs (open squares) are shown in Fig. 17 in the diagram (a) "M_{Ks} vs. Fe/H", (b) "$(J-Ks)$ vs. Fe/H". The relation for ESDs is due to 2 most

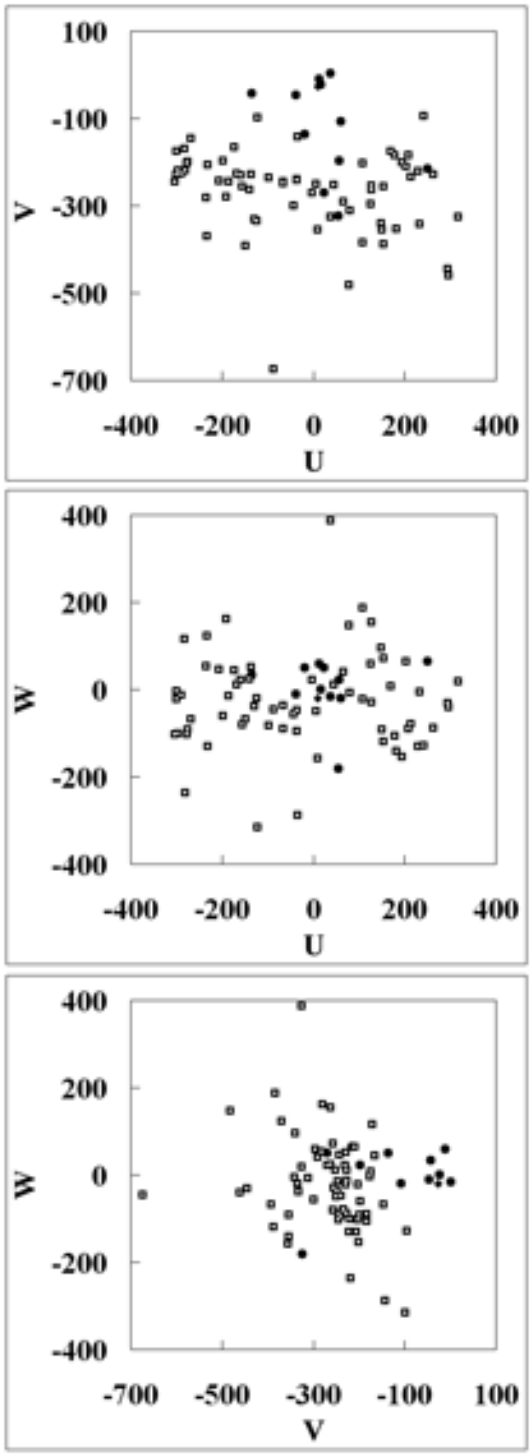

Figure 15: The distribution of WD (diamond), ESDs (circles) and USDs (open squares) with precise RVs in the projection to the UV, UW and VW planes (velocities in km s^{-1}).

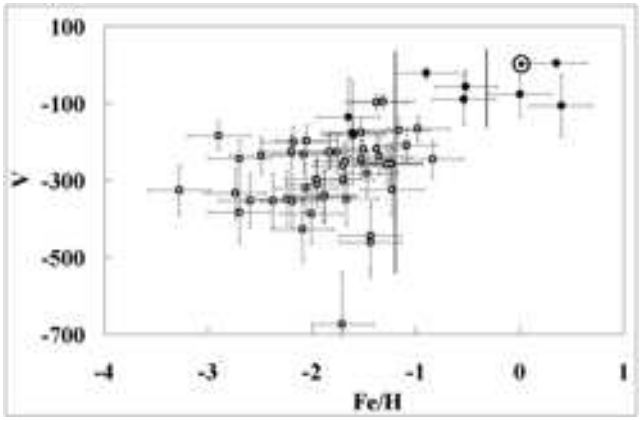

Figure 16: The relation of the Fe/H and velocity component V for ESDs (circles) and USDs (open squares).

luminous stars mentioned above with high velocity and low metallicity. The relations for the USDs can be explained by "$(J-Ks)$ – age" and "$(J-Ks)$ – metallicity" relations [Girardi et al., 2000]: the turn-off point becomes redder with rise of the age and metallicity. Therefore, one can see that the redder part of the USD subsample contains old stars with moderate metallicity whereas the bluer part has larger dispersion of the Fe/H because of the admixtures of younger stars with higher Fe/H as well as older stars with lower Fe/H.

The galactic orbits are calculated for 183 selected stars with XYZUVW set accepting the solar galactocentric distance of 8.5 kpc. The model of the gravitational potential of the Galaxy by [Allen & Santillán, 1991] is adopted. The orbits were calculated over a total of 1.1 Gyr backwards.

The eccentricities for 3 WDs are 0.05 for 2MASS PSC 1098632336, 0.12 for HIP 14754 and 0.36 for HIP 101516. The projections of the WD orbits into XY, XZ and YZ planes are shown in Fig. 18, row (a) by solid, dotted and dashed curves for different stars (distances in kpc). All of these orbits better fit to the thin disk.

The mean eccentricity for 41 ESDs is 0.46 ± 0.3 and the one for 139 USDs is 0.8 ± 0.2. The projections of the ESD and USD orbits into XY, XZ, YZ planes are shown in Fig. 18, rows (b) and (c) respectively (distances in kpc). One should pay attention to the different scales in the subfigures.

The distributions of ESDs (dashed line) and USDs (solid line) on the orbital eccentricity and apogalactic distance Zmax are shown in Fig. 19 (a) and (b) respectively. The vertical lines show suspected separation into thin disk, thick disk and halo.

In Fig. 20 we show the average spatial distribution of ESDs (dashed line) and USDs (solid line) on Z distance (in kpc) based on their orbits. It is given by the statistics of the orbital points calculated with equal time steps of 1 Myr. It is similar to the analysis of the galactic orbits of sdB stellar sample by [de Boer et al., 1997]. In contrast to them, our results expand far beyond $|Z| = 4$ kpc and our distributions do not have local minima at Z=0. The reason of the difference is that their choice of stars was solely determined by the availability of the data giving some selection. But our sample is deeper, and near the Sun it is almost complete without any selection. Within $|Z| < 2.5$ kpc both ESD and USD samples are dominated by the thick disk stars. Their spatial distribution in Z is fairly the same for ESDs and USDs and fits an exponential distribution with a scale height of about 1.25 ± 0.1 kpc. The wings of

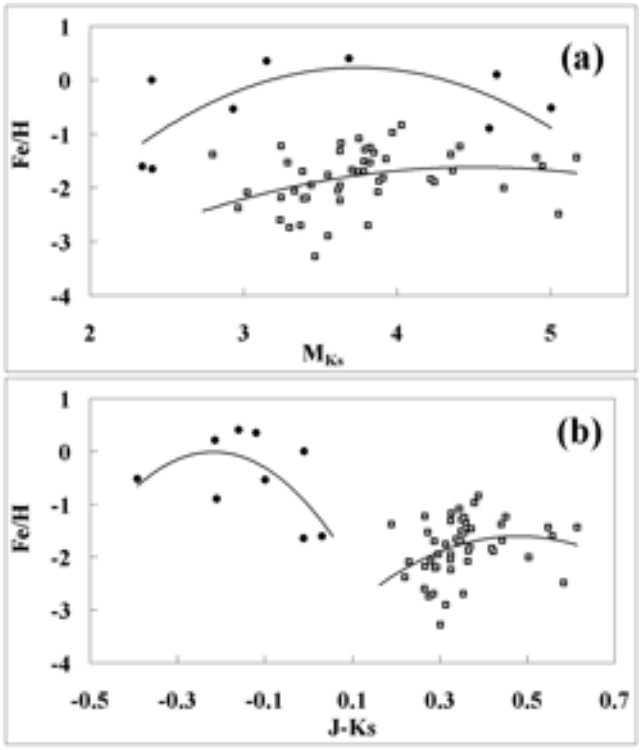

Figure 17: The relation of the Fe/H and (a) M_{Ks}, (b) $(J-Ks)$ for ESDs (circles) and USDs (open squares).

the distributions are populated by the halo ESD and USD stars. The halo ESDs are rare and show no distribution low. The USD halo spatial distribution in Z fits an exponential one with a scale height of about 8 ± 1 kpc. Our USD halo is so well-defined that we can calculate its local mass density assuming mean stellar mass of $0.5 M_{\odot}$: $\rho_0 = 2 \cdot 10^{-5} M_{\odot}\ pc^{-3}$. It is nearly 2 times higher than the local mass density for all halo star accepted for the Besançon model of the Galaxy by [Robin et al., 2003], although the Besançon value is initial mass function dependent. This density increase may be due to our sample depth and completeness.

The relations of Fe/H versus eccentricity, perigalactic distance Rmin (in kpc) and apogalactic distance Rmax (in kpc) are shown in Fig. 21 (a), (b) and (c) respectively for ESDs (circles) and USDs (open squares). It is evident that 2 ESD outliers mentioned above have halo member properties similar to the USDs. The rest ESDs show the properties of disk members.

The conclusions from the Fig. 19, 20 and 21 are the same: most ESDs belong to thick disk whereas most USDs belong to halo.

7 Catalogue format

The properties of the 9799 selected stars are presented in electronic form as the catalogue "Subdwarfs and white dwarfs from the 2MASS, Tycho-2, XPM and UCAC3 catalogues" (hereafter SDWD catalogue). The table 3 gives its format. The catalogue data are arranged by the stellar class from 1 (WD) to 2 (ESD) and 3 (USD) as well as obtained M_{Ks} increasing within the class).

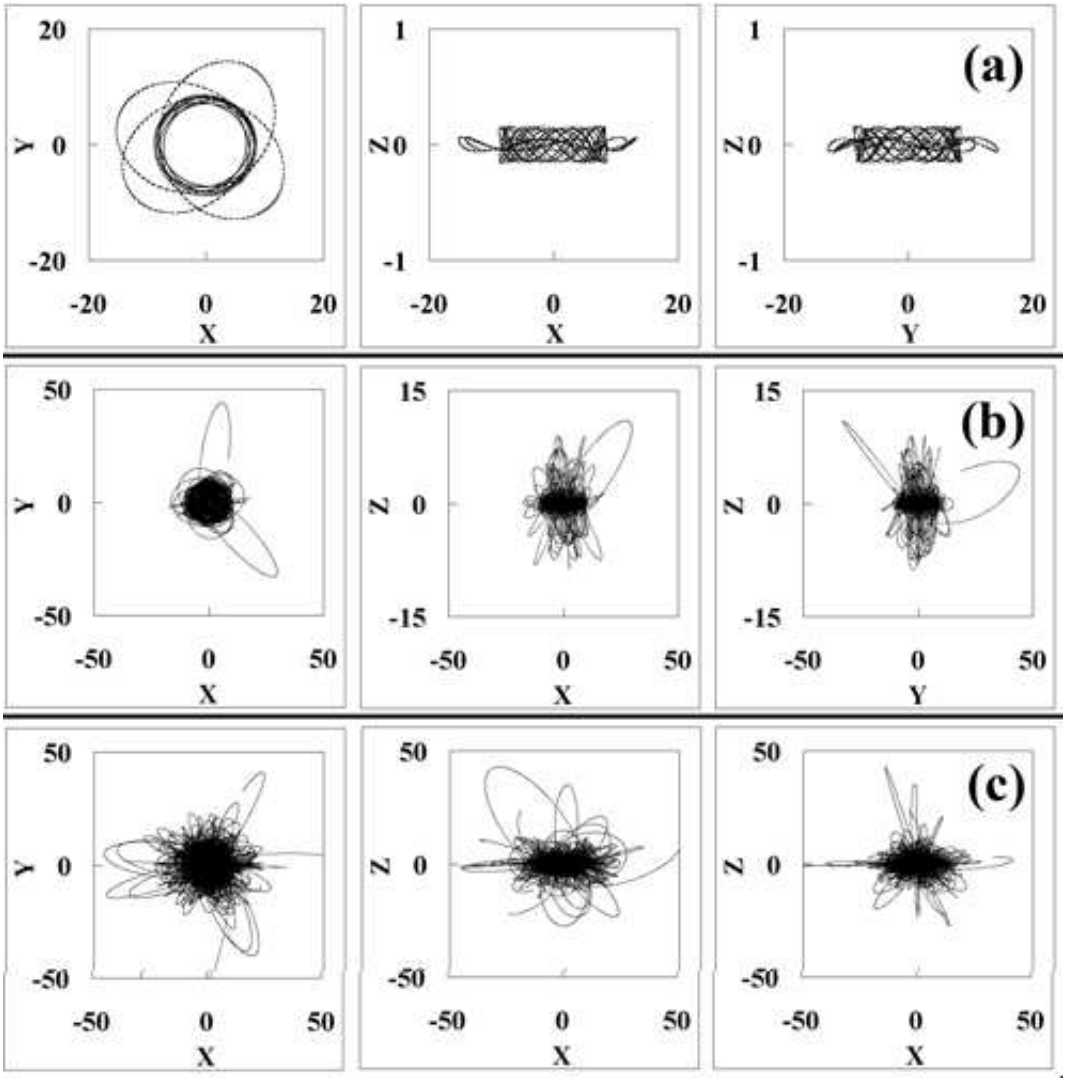

Figure 18: The projections of the (a) WD, (b) ESD and (c) USD orbits into XY, XZ and YZ planes. The scales are different.

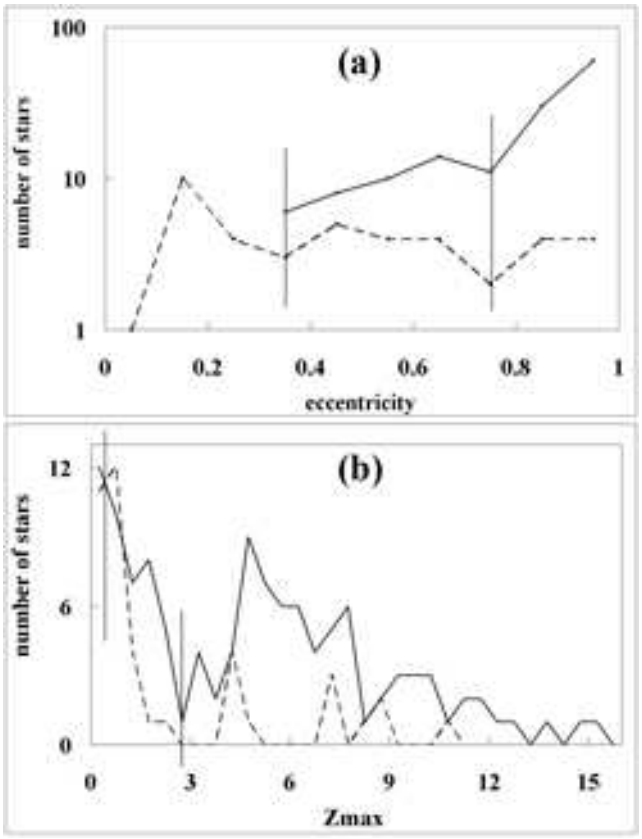

Figure 19: The distribution of ESDs (dashed line) and USDs (solid line) (a) on orbital eccentricity and (b) on apogalactic distance Zmax. The vertical lines show suspected separation into thin disk, thick disk and halo.

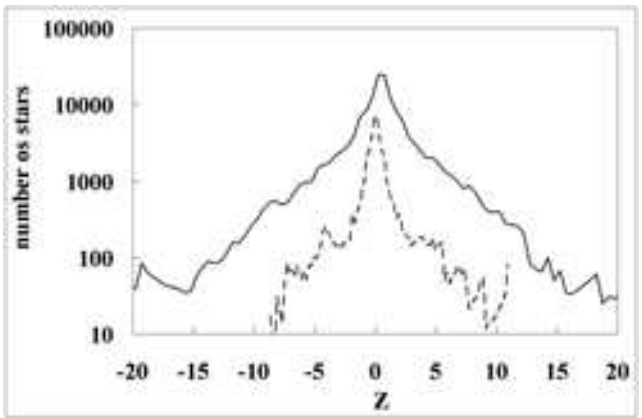

Figure 20: The average spatial distribution of ESDs (dashed line) and USDs (solid line) on Z distance (in kpc) based on their orbits.

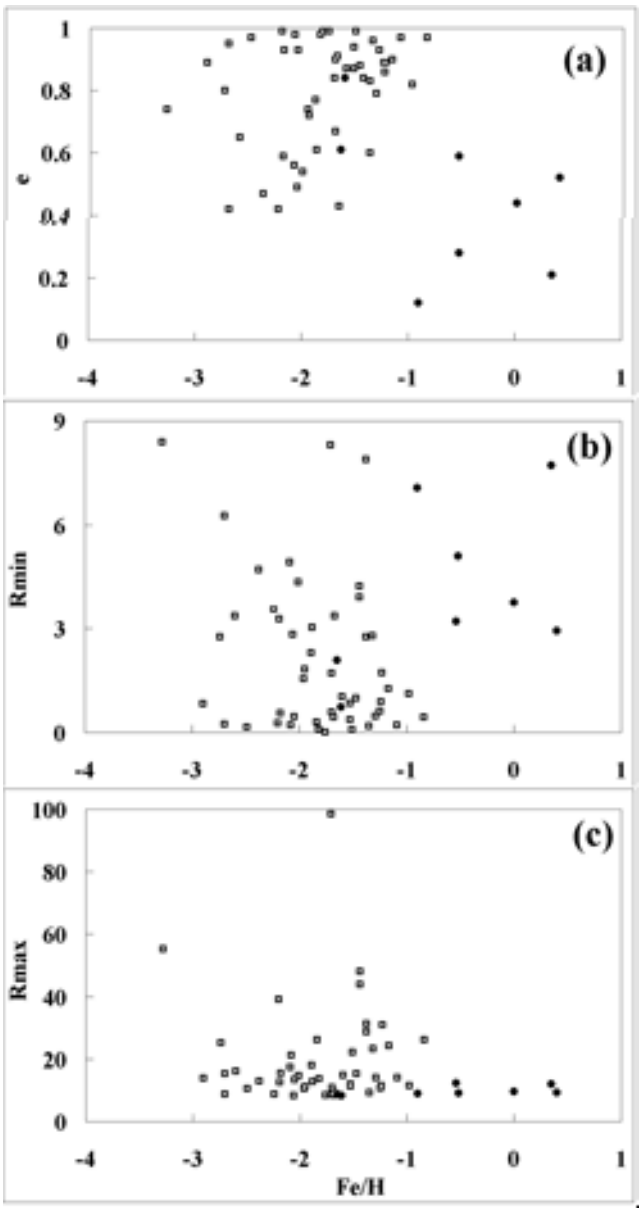

Figure 21: The relations of Fe/H versus eccentricity, perigalactic and apogalactic distance (in kpc) for ESDs (circles) and USDs (open squares).

Table 3: Format of the catalogue of subdwarfs and white dwarfs from the 2MASS, Tycho-2, XPM and UCAC3.

field	format	positions
2MASS psc number	I10	1-10
Tycho-2 number	A10	11-20
Hipparcos number	I6	21-26
stellar class (WD=1, ESD=2, USD=3)	I1	27-27
obtained M_{Ks}	F5.2	28-32
l in decimal degs	F8.4	33-40
b in decimal degs	F8.4	41-48
$\mu_l \cos(b)$ in mas yr^{-1}	F7.1	49-55
μ_b in mas yr^{-1}	F7.1	56-62
Hipparcos parallax in mas	F6.2	63-68
parallax precision in mas	F4.1	69-72
B_T mag from Tycho-2	F5.2	73-77
B_T precision from Tycho-2	F4.2	78-81
V_T mag from Tycho-2	F5.2	82-86
V_T precision from Tycho-2	F4.2	87-90
J mag from 2MASS	F5.2	91-95
Ks mag from 2MASS	F5.2	96-100
R_{UCAC3} mag from UCAC3	F5.2	101-105
R_{UCAC3} precision from UCAC3	F4.2	106-109
B_{SC} mag from SuperCosmos	F5.2	110-114
R_{SC} mag from SuperCosmos	F5.2	115-119
I_{SC} mag from SuperCosmos	F5.2	120-124
B_{SC} quality flag from UCAC3	I1	125-125
R_{SC} quality flag from UCAC3	I1	126-126
I_{SC} quality flag from UCAC3	I1	127-127
obtained photometric distance in pc	I4	128-131
obtained X distance in pc	I5	132-136
obtained Y distance in pc	I5	137-141
obtained Z distance in pc	I5	141-146
radial velocity in km s^{-1}	F6.1	147-152
RV precision in km s^{-1}	I2	153-154
Fe/H	F4.1	155-158
epoch difference from XPM in years	F5.2	159-163
velocity component U in km s^{-1}	F6.1	164-169
velocity component V in km s^{-1}	F6.1	170-175
velocity component W in km s^{-1}	F6.1	176-181
apogalactic distance in kpc	F4.1	182-185
perigalactic distance in kpc	F3.1	186-188
galactic orbit eccentricity	F4.2	189-192

8 Conclusions

New all-sky astrometric and photometric surveys (2MASS, XPM, UCAC3, SuperCosmos, Tycho-2) appear suitable to make the largest sample of subluminous stars candidates: 7769 unevolved subdwarfs, 1996 evolved subdwarfs and 34 white dwarfs. The key feature of this selection is the detailed analysis of the distribution of all stars from these catalogues in the various "color index vs. reduced proper motion" planes as well as Monte-Carlo simulation of this distribution. It is found that only surveys with proper motion accuracy better than 10 mas yr^{-1} provide the acceptable separation of the subluminous stars from the main sequence, while with 10% admixture and considerable selection biases in favor to faster stars. It is proved that most of the Tycho-2, XPM and UCAC3 stars fit this criterion of the proper motion accuracy. It is pointed out that future surveys with proper motion accuracy better than 1 mas yr^{-1} can provide a perfect separation without an admixture and bias. The multi-color photometry also appears useful for the subluminous star selection and separation of evolved and unevolved subdwarfs as well as single and binary stars. It is pointed out that current level of the photometric accuracy is acceptable for such tasks but the level of about 0.01^m is desirable for better separation.

The calibrations "color index vs. absolute magnitude" and "reduced proper motion vs. absolute magnitude" made with the best Hipparcos stars allow us to calculate photometric and photoastrometric distances for all the selected stars, consider their 3D distribution, while complete only near the Sun. The use of radial velocities for 183 stars and Fe/H metallicities for 56 stars allow us to consider their 3D motion and metallicity-velocity relation.

This investigation tests some theories related to the subluminous stars. Namely, it is shown that unevolved and evolved subdwarfs have different evolutionary status, kinematics and metallicity. The most USDs are population II low metallicity high asymmetric drift stars from halo with the scale height of 8 ± 1 kpc and local mass density of the halo USDs of $2 \cdot 10^{-5} M_\odot\ pc^{-3}$. The ESDs are a heterogeneous group containing stars from disk and halo with metallicities from low to solar one and with halo to thin disk kinematics. However, most evolved subdwarfs seems to belong to thick disk with scale height of 1.25 ± 0.1 kpc. The evolved subdwarfs appear the most interesting group. They show some spatial overdensities of yet unknown nature, large fraction of binaries and vast diversity of properties not all of which have been explained by current theories.

All important parameters of the selected stars are compiled into the SDWD catalogue in order to continue their investigations, specially to prove their status by spectroscopy.

9 ACKNOWLEDGMENTS

This study was supported by the Fundamental Researches State Fund of Ukraine (project No. FRSF-28/238) and the Russian Foundation for Basic Research (projects No. 08-02-00400 and No. 09-02-90443-Ukr-f), and in part by the "Origin and Evolution of Stars and Galaxies" - "Program of the Presidium of the Russian Academy of Sciences and the Program for State Support of Leading Scientific Schools of Russia" (NSh-6110.2008.2).

References

[Allen & Santillán, 1991] Allen C., Santillán A., 1991, Rev. Mexicana Astron. Astrof., 22, 255

[Bertelli et al., 2008] Bertelli G., Girardi L., Marigo P., Nasi E., 2008, A&A, 484, 815

[de Boer et al., 1997] de Boer K.S., Aguilar Sanchez Y., Altmann M., Geffert M., Odenkirchen M., Schmidt J.H.K., Colin J., 1997, A&A, 327, 577

[Cassisi et al., 2003] Cassisi, S., Schlattl G., Salaris M., Weiss A., 2003, APJ, 582, L43

[Catelan, 2007] Catelan, M., 2007, American Institute of Physics Conf. Proc., 930, 39

[Fagotto et al., 1994] Fagotto, F., Bressan A., Bertelli G., Chiosi C., 1994, A&AS, 104, 365

[Fedorov, Myznikov & Akhmetov, 2009] Fedorov P.N., Myznikov A.A., Akhmetov V.S., 2009, MNRAS, 393, 133

[Fedorov et al., 2010] Fedorov P.N., Akhmetov V.S., Bobylev V.V., Bajkova A.T., 2010, MNRAS, in press

[Finlator et al., 2000] Finlator K., Ivezic Z., Fan X., et al., 2000, AJ, 120, 2615

[Girardi et al., 2000] Girardi L., Bressan A., Bertelli G., Chiosi C., 2000, A&AS, 141, 371

[Girardi et al., 2005] Girardi L., Groenewegen M.A.T., Hatziminaoglou E., da Costa L., 2005, A&A, 436, 895

[Gontcharov, 2006] Gontcharov G.A., 2006, Astronomy Letters, 32, 759

[Gontcharov, 2008a] Gontcharov G.A., 2008a, Astronomy Letters, 34, 7

[Gontcharov, 2008b] Gontcharov G.A., 2008b, Astronomy Letters, 34, 868

[Gontcharov, 2009a] Gontcharov G.A., 2009a, Astronomy Letters, 35, 707

[Gontcharov, 2009b] Gontcharov G.A., 2009b, Astronomy Letters, 35, 862

[Hambly, Irwin & MacGillivray, 2001] Hambly N.C., Irwin M.J., MacGillivray H.T., 2001, MNRAS, 326, 1295

[Han et al., 2003] Han Z., Podsiadlowski Ph., Maxted P.F.L., Marsh T.R., 2003, MNRAS, 341, 669

[Hipparcos and Tycho catalogues, 1997] Hipparcos and Tycho catalogues, 1997. ESA

[Høg et al., 2000] Høg E., Fabricius C., Makarov V.V., et al., 2000, A&A, 355, L27

[Jones, 1972] Jones E.M., 1972, APJ, 173, 671

[van Leeuwen, 2007] van Leeuwen F., 2007, A&A, 474, 653

[Miller Bertolami et al., 2008] Miller Bertolami M.M., Althaus L.G., Unglaub K., Weiss A., 2008, A&A, 491, 253

[Monet, 1998] Monet D., 1998, BAAS, 30, 1427

[Østensen, 2009] Østensen, 2009, in Schuh S. & Handler G., eds., Proc. JENAM 2008 Symp. #4, Asteroseismology and Stellar Evolution, 159, 75

[Robin et al., 2003] Robin A.C., Reyle C., Derriere S., Picaud S., 2003, A&A, 409, 523

[Skrutskie et al., 2006] Skrutskie M.F., Cutri R.M., Stiening R., et al., 2006, ApJ, 131, 1163

[Smith et al., 2009] Smith M.C., Evans N.W., Belokurov V., et al., 2009, MNRAS, 399, 1223

[Stark & Wade, 2003] Stark M.A., Wade R.A., 2003, AJ, 126, 1455

[Vassiliadis & Wood, 1994] Vassiliadis E., Wood P.R., 1994, ApJS, 92, 125

[Veltz et al., 2008] Veltz L., Bienayme O., Freeman K.C., et al., 2008, A&A, 480, 753

[Wichman & Hill, 1982] Wichman B.A., Hill I.D., 1982, Applied Statistics, 31, 188

[Wright et al., 2003] Wright C.O., Egan M.P., Kraemer K.E., Price S.D., et al., 2003, AJ, 125, 359

[Zacharias et al., 2009] Zacharias N., et al., 2009, AJ, in press